J Shoulder Elbow Surg (2021) 30, 747–755

ELSEVIER

Journal of Shoulder and Elbow Surgery

www.elsevier.com/locate/ymse

Humeral intramedullary nail placement through the rotator interval: an anatomic and radiographic analysis

Eliana B. Saltzman, MD[a,*], Elshaday Belay, MD[a], Andrew E. Federer, MD[a], Robert French, MD[b], Oke Anakwenze, MD, MBA[a], Mark J. Gage, MD[a], Christopher S. Klifto, MD[a]

[a]*Department of Orthopedic Surgery, Duke University Medical Center, Durham, NC, USA*
[b]*Department of Radiology, Duke University Medical Center, Durham, NC, USA*

Background: Antegrade humeral intramedullary nails are an effective fixation method for certain proximal humeral fractures and humeral shaft fractures. However, owing to potential rotator cuff damage during nail insertion, shoulder pain remains a common postoperative complaint. The purpose of this study was to provide quantitative data characterizing the anatomic and radiographic location of the rotator interval (RI) for an antegrade humeral intramedullary nail using a mini-deltopectoral approach.

Methods: Six consecutive fresh-frozen intact cadaveric specimens (mean age, 69 ± 12.8 years) were obtained for our study. Demographic data were collected on each specimen. A mini-deltopectoral approach was used, followed by placement of a guidewire in the RI. Quantitative anatomic relationships were calculated using a fractional carbon fiber digital caliper. Radiographic measurements were performed by 2 orthopedic residents and 1 practicing fellowship-trained orthopedic surgeon. In addition to re-measurement of similar anatomic relationships on radiographs, the ratio of the distance from the lateral humeral edge to the starting point relative to the width of the humeral head on the anteroposterior (AP) view was calculated. Similarly, on the lateral view, the ratio of the distance from the anterior humeral edge to the starting point relative to the humeral head width was calculated.

Results: In all cases, the described approach allowed for preservation of the biceps tendon and access to the RI for guidewire insertion, with no subsequent rotator cuff or humeral articular cartilage damage identified following nail insertion. The ratio of the distance from the lateral humeral edge to the starting point relative to the humeral head width on the AP view was 0.4 ± 0.0. The ratio of the distance from the anterior humeral edge to the starting point relative to the humeral head width on the lateral view was 0.3 ± 0.0.

Conclusion: This study demonstrates the clinical feasibility of a mini-deltopectoral approach and shows that the ideal starting point through the RI radiographically lies along the medial aspect of the lateral third of the humeral head on the AP view and along the posterior aspect of the anterior third of the humeral head on the lateral view.

Level of evidence: Anatomy Study; Cadaveric Dissection and Imaging

Keywords: Humerus; fracture; proximal; diaphyseal; intramedullary nail; rotator interval

Institutional review board approval was received from Duke University Medical Center (Pro00105411).

*Reprint requests: Eliana B. Saltzman, MD, Department of Orthopaedic Surgery, Duke University Medical Center, Box 104002, Durham, NC 27710, USA.

E-mail address: eliana.saltzman@duke.edu (E.B. Saltzman).

1058-2746/$ - see front matter © 2020 Journal of Shoulder and Elbow Surgery Board of Trustees. All rights reserved.
https://doi.org/10.1016/j.jse.2020.07.044

Humeral fractures account for up to 8% of all fractures, with the incidence of humeral shaft fractures being 13 per 100,000 person-years.[4,6] Furthermore, proximal humeral fractures are the third most common fracture in patients aged > 65 years, with emergency department visits projected to exceed 275,000 annually by 2030.[18] Surgical treatment of these fractures continues to be challenging despite several treatment options currently available.

Open reduction–internal plate fixation is typically performed using extensile exposure to allow for direct visualization of fracture reduction, whereas intramedullary nail (IMN) fixation typically involves implantation with more limited surgical exposure and potentially less soft tissue dissection. Currently, the superior fixation strategy for humeral fractures remains unclear. In a randomized controlled trial by Gracitelli et al,[7] IMNs and locked plating were shown to have similar radiographic union results, although IMNs had higher rates of complication and reoperation. A recent American Board of Orthopaedic Surgery case database demonstrated a decrease in complication rates of IMN fixation without a significant difference in nonunion rates, and a subsequent meta-analysis concluded that IMNs were superior to locked plate fixation in maintaining overall length, as well as decreasing blood loss, operative time, and fracture healing time.[13] Despite this, a significant deterrent to humeral nailing is the potential shoulder stiffness and pain described postoperatively due to rotator cuff tendinopathy from the surgical approach.

The rotator interval (RI), first named by Neer[16] in 1970, consisting of the anterior capsule, coracohumeral ligament, and superior glenohumeral ligament, is an anatomic location bridging the supraspinatus and subscapularis tendons.[9,20] Specifically, this triangular interval is bordered by the subscapularis anteroinferiorly, supraspinatus posterosuperiorly, and coracoid medially. Previous cadaveric and arthroscopic studies have described the macroscopic constituents of the RI.[12] This landmark is readily available and easily accessed during both open and arthroscopic shoulder surgical procedures. The potential of accessing the humeral proximal body and shaft using this interval and therefore sparing the rotator cuff tendons creates an opportunity to possibly lower the rate of shoulder pain after humeral IMN fixation.

Therefore, the purpose of this study was to provide quantitative data characterizing the anatomic and radiographic location of the RI to be used for placement of antegrade humeral IMNs, an inherently more medial and anterior starting point compared with the traditional approach, to reduce injury to the rotator cuff tendon.

Table I Cadaveric demographic data

Variable	Data
Age, mean ± SD, yr	69 ± 12.8
Male sex, n	3
Humeral length from GT to LE, mean ± SD, cm	33.7 ± 1.8
Humeral length from acromion to LE, mean ± SD, cm	36.8 ± 2.4
Arm length from GT to distal phalanx of long finger, mean ± SD, cm	82.3 ± 1.8

SD, standard deviation; *GT*, greater tuberosity; *LE*, lateral epicondyle.

Materials and methods

Overview

This study was conducted according to standard procedures for handling human fresh tissue. Six consecutive fresh-frozen intact cadaveric specimens (entire bodies) were obtained for our study. Demographic data were collected on each specimen, including age, sex, and race.

Specimen information

To determine the anatomic and radiographic landmarks of the RI and humeral nail starting point, we examined 3 paired, fresh-frozen human cadavers (Table I). All 3 cadavers were male, with an average age of 69 ± 12.8 years. The average antebrachial arm length, measured from the greater tuberosity to the lateral epicondyle, was 33.7 ± 1.8 cm. The average arm length, measured from the greater tuberosity to the distal phalanx of the long finger, was 82.3 ± 1.8 cm. Shoulders with a history of surgery or ligamentous injury were excluded. None of the specimens were found to have a rotator cuff tear, and all specimens had an intact long head of the biceps tendon.

Anatomic dissection

The specimens were placed in the beach-chair position, with bed inclination of 45°, and a mini-deltopectoral approach was used. For each specimen, a 4-cm-long incision was made, extending from the coracoid process (Fig. 1, *A*). The cephalic vein was preserved in all cases and retracted laterally (Fig. 1, *B*). The clavipectoral fascia was incised. The biceps tendon was next identified in the bicipital groove, and the proximal aspect of the transverse humeral ligament was released, allowing the biceps tendon to be dislocated medially without being fully released (Fig. 2, *A* and *B*). The superior insertion of the subscapularis was defined, as was the anterior edge of the supraspinatus tendon. Finally, a small portion of the coracohumeral ligament was released, with care taken to preserve the coracoacromial ligament (Fig. 2, *C*). After completion of the anatomic dissection, radiographic T-pin markers were placed on the coracoid process,

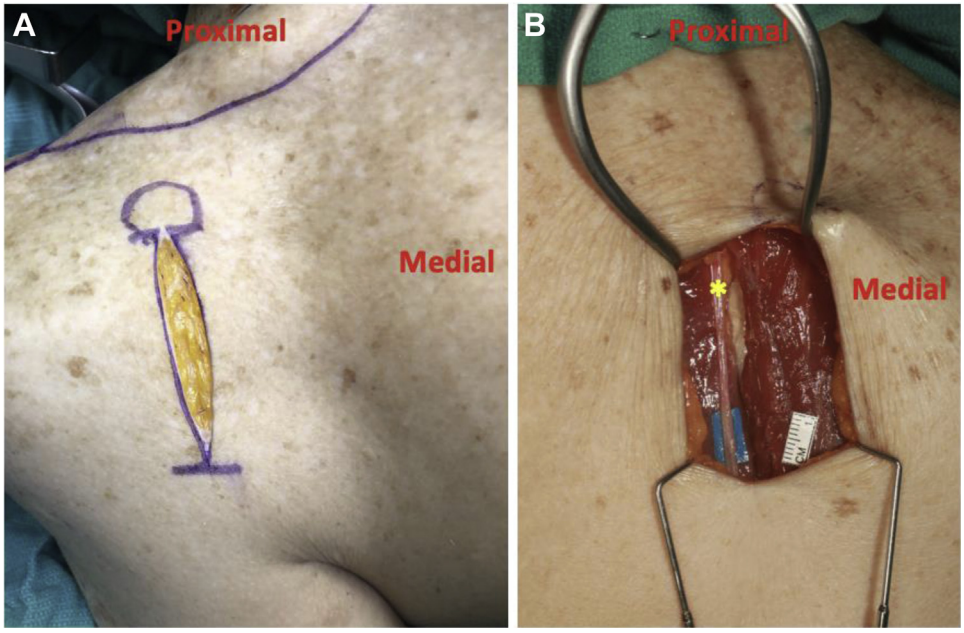

Figure 1 Deltopectoral approach demonstrating initial incision (**A**) and cephalic vein (*) (**B**).

anterior edge of the supraspinatus, and insertion of the subscapularis (Fig. 3).

Quantitative anatomy

Anatomic landmarks were measured using a fractional carbon fiber digital caliper. Tendon attachments, osseous landmarks, and the glenohumeral joint were manually identified. The RI was calculated as the mean surface volume using the Heron formula: Area $= \sqrt{s(s-a)(s-b)(s-c)}$.[17] Area and distance measurements were reported as means. Furthermore, the ratio of the distance from the lateral humeral edge to the starting point relative to the humeral head width on the anteroposterior (AP) view was calculated. This ratio was replicated on the lateral view, in which the ratio of the distance from the anterior humeral edge to the starting point relative to the humeral head width was calculated.

Radiography

A guidewire was placed through the center of the RI in an AP direction under fluoroscopic guidance (Fig. 4). The guidewire was directed in line with the humeral diaphysis on AP, lateral, and axial fluoroscopic views (Fig. 5). A true AP glenoid radiograph (Grashey view) was confirmed when the glenohumeral joint was open and the anterior and posterior aspects of the glenoid were superimposed. Additionally, determination of the radiographic starting point was further aided by obtaining a bicipital groove view. To obtain this view, the fluoroscopic C-arm was first placed over the shoulder and centered to obtain an accurate AP glenoid (Grashey) view. Then, to obtain the bicipital groove view (Fig. 5, *B*), the humerus was placed in 30° of abduction and 45° of external rotation. A 25.4-mm radiopaque sphere (diameter, 25.4 ± 0.00254 mm; sphericity, 0.00061 mm) was positioned in the field of view, at the level of the identified structures, to correct for magnification disparities and allow for calibration of images during subsequent measurements. Radiographs were imported into a picture archiving and communication system (PACS) program (eUnity workstation, version 6.7.1-1564; Client Outlook, Waterloo, ON, Canada) for digital radiographic measurements.

Three observers performed the radiographic measurements: 2 orthopedic residents and 1 practicing fellowship-trained orthopedic surgeon. Measurements were reported as means and standard deviations.

IMN placement

A 10-mm reamer was used to open the humerus proximally while the biceps tendon was carefully retracted medially, and an 8-mm × 200-mm nail with a 9° lateral bend (Polarus humeral nail; Acumed, Hillsboro OR, USA) was inserted in the standard fashion (Fig. 6). Once the nail was placed, it was removed, and the integrity of the rotator cuff and articular cartilage was examined for changes in tissue and articular quality.

Results

Quantitatively, the mean RI surface area was 281.2 ± 68.6 mm^2, and the mean bicipital groove width was 4.8 ± 1.2 mm (Table II). The distance from the starting point to the edge of the subscapularis and supraspinatus was 6.5 ± 0.9 mm and 4.9 ± 0.6 mm, respectively. Additional anatomic measurements are presented in Table II.

Radiographically, the mean distance from the starting point to the medial edge of the bicipital groove was 5.9 ± 0.3 mm (Table III). The distance from the starting point to the edge of the subscapularis and supraspinatus was 8.8 ± 0.5 mm and 7.4 ± 0.4 mm, respectively. The ratio of the

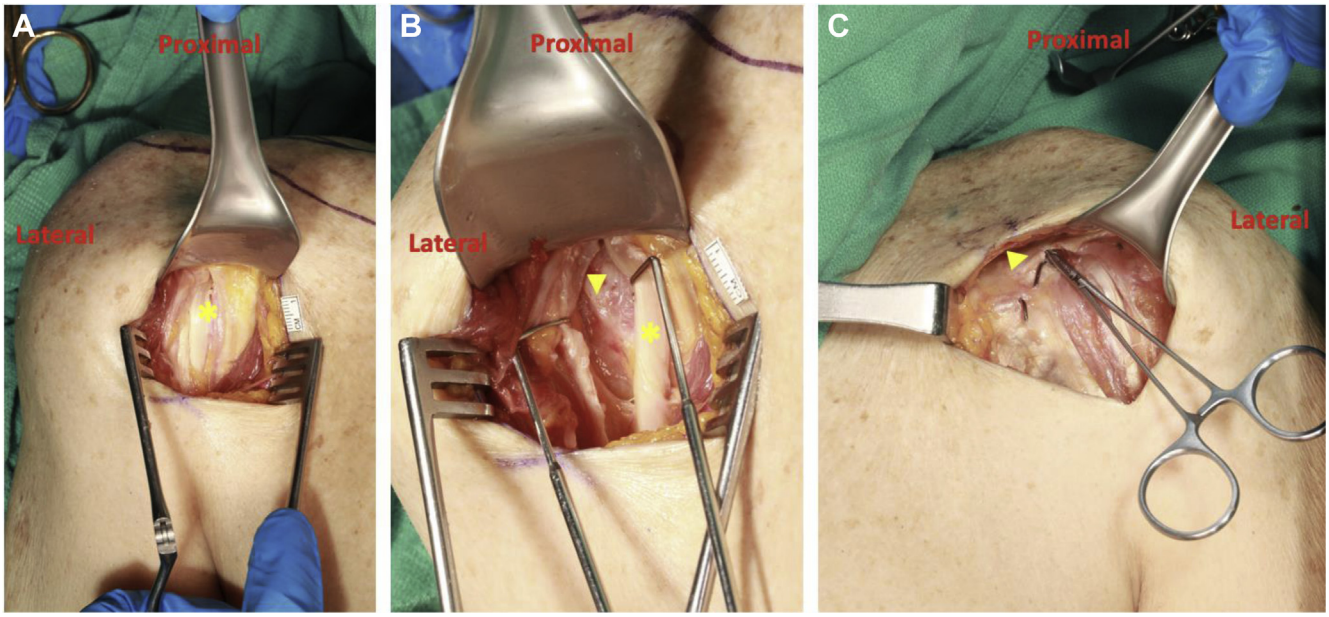

Figure 2 (**A**) Further dissection with biceps tendon (*) within bicipital groove and transverse humeral ligament incised. (**B**) The biceps tendon (*) is dislocated medially, exposing the bicipital groove (◀). (**C**) The coracohumeral ligament (*) is snipped to expose the guidewire starting point.

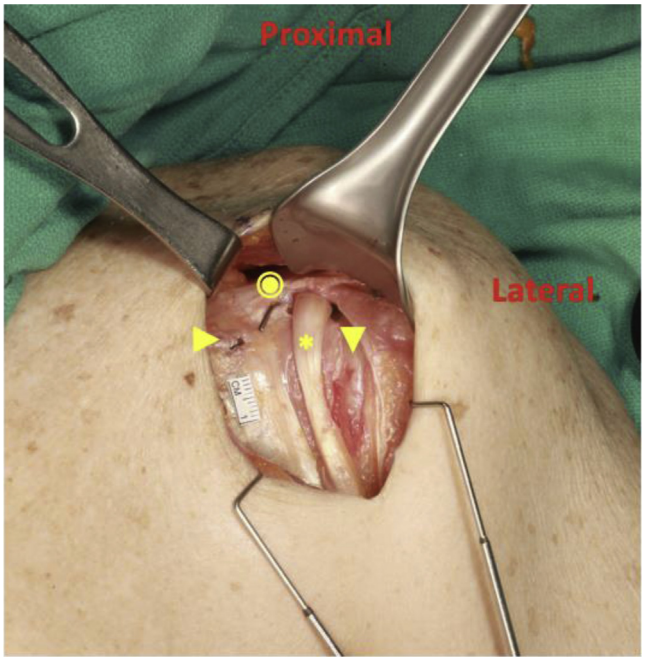

Figure 3 Final dissection prior to guidewire placement. The ▼ indicates the coracoid; ◯, subscapularis insertion; *, biceps tendon medially dislocated; and ◀, bicipital groove.

distance from the lateral humeral edge to the starting point relative to the humeral head width on the AP view was 0.4 ± 0.0. The ratio of the distance from the anterior humeral edge to the starting point relative to the humeral head width on the lateral view was 0.3 ± 0.0 (Table IV). Following nail insertion, we found the rotator cuff and humeral articular cartilage to be intact (Fig. 7).

Discussion

Postoperative shoulder dysfunction is a continuing concern with humeral nailing. We present an approach to humeral nailing through the RI that minimizes the potential for damage to critical structures in the shoulder. We have further delineated the starting point both anatomically and radiographically to allow for reproducibility in surgical executions. It is, to our knowledge, the first description of a humeral nailing starting point through the RI using a deltopectoral approach.

Shoulder dysfunction following antegrade humeral IMN fixation remains the most common and significant postoperative complication. Postoperative shoulder adverse events include impingement, decreased range of motion, and adhesive capsulitis. This may be due in part to implant prominence, postoperative scarring, or iatrogenic rotator cuff tendon injury. The rate of shoulder dysfunction postoperatively ranges between 10% and 20%.[1,2,15,23] It is interesting to note that in one study using ultrasound to evaluate the rotator cuff postoperatively, 44 of 48 patients had no evidence of supraspinatus injury.[22] Furthermore, no correlation was found between ultrasound findings and Constant scores. Here, we present a starting point that is sufficiently medial and anterior to avoid the posterior-superior rotator cuff tendons and footprint to hopefully avoid these postoperative complications.

The early humeral nails were curvilinear in shape and designed for insertion through a lateral entry point to avoid articular injury. Unfortunately, this in turn led to iatrogenic injury to the rotator cuff tendon and postoperative pain.[21]

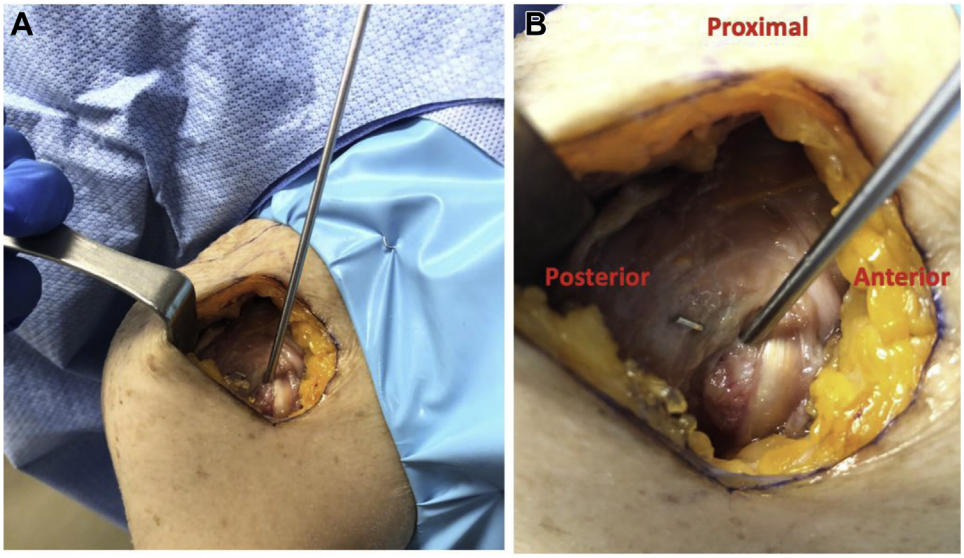

Figure 4 (**A**) Cadaveric dissection demonstration of humeral intramedullary nail starting point. (**B**) Further visualization of starting point within rotator interval and guidewire placed at apex of humeral head convexity.

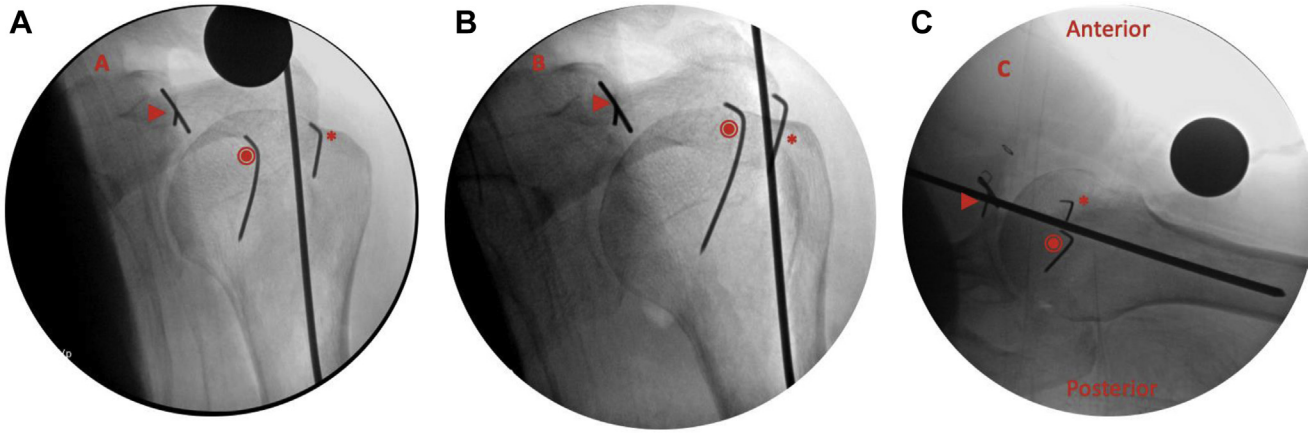

Figure 5 Radiographic illustration: anteroposterior glenoid view (**A**), bicipital groove view (**B**), and lateral view (**C**) with guidewire advanced to humeral diaphysis. The ▶ indicates the coracoid; ●, subscapularis insertion; and *, supraspinatus insertion.

Lopiz et al[14] found that rotator cuff symptoms developed in 73% of patients treated with curved nails compared with 34.6% of those treated with straight nails. Additionally, a significantly higher revision rate of 42% was seen in the bent-nail cohort (9° bend) compared with 11.5% in patients with straight nails. Unlike curvilinear nail designs, straight nail designs allow for a more medial entry point from the footprint and central placement in the humeral head.[21] Straight nails have also been shown to preserve the surrounding bone stock, aiding in the biomechanical stability and anchoring of the implant.[8] Although straight nails better protect the rotator cuff tendon and footprint, they do require violation of the humeral head articular cartilage.[21]

Optimal placement of the humeral IMN can be technically challenging. An improper and excessively lateral starting point can lead to significant rotator cuff tendon insertional damage. A lateral deltoid-splitting approach is most commonly used for IMN placement. We have proposed using a mini-deltopectoral approach. The advantages include ease of incisional extension for improved visualization without risk of axillary nerve injury, improved visualization of the rotator cuff footprint and lateral edge of the humeral head articular surface, and a more conducive approach for glenoid exposure if a subsequent revision operation is required. This approach further takes advantage of the improvements in the straight humeral IMN design, allowing for minimized trauma to the rotator cuff tendon and the humeral head articular surface.

Christ et al[3] in 2017 described an approach for antegrade humeral nailing through the RI that avoided rotator cuff splitting with concomitant tenodesis of the long head of the

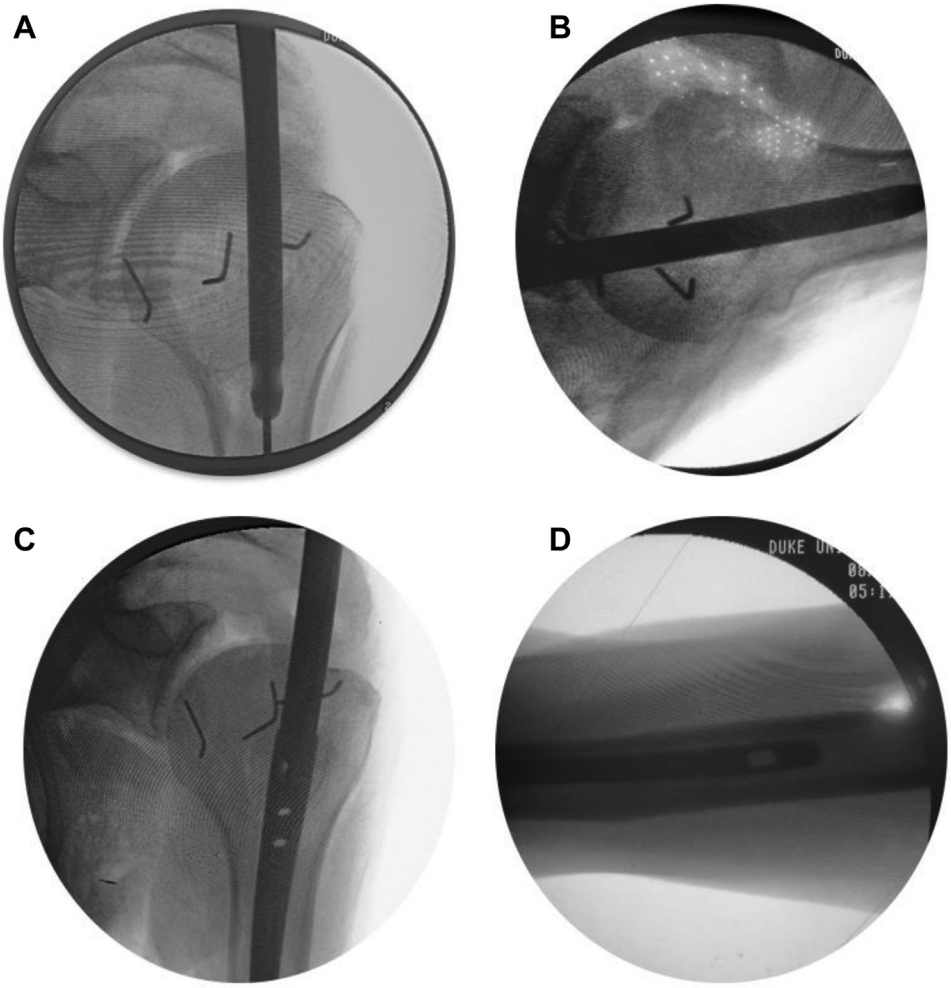

Figure 6 Radiographic images of humeral nail placement: anteroposterior view of humeral nail insertion (**A**), lateral view of humeral nail insertion (**B**), anteroposterior view of proximal humeral stem (**C**), and lateral view of distal end of humeral nail (**D**).

Table II Anatomic measurements

Anatomic measurement	Mean ± SD
Rotator interval area, mm^2	281.2 ± 68.6
Bicipital groove width, mm	4.6 ± 1.2
Distance from starting point to ACJ, mm	59.2 ± 3.5
Distance from starting point to coracoid, mm	25.6 ± 3.5
Distance from starting point to center of GT, mm	32.3 ± 4.4
Distance from starting point to lateral articular edge of humerus, mm	5.3 ± 1.9
Distance from starting point to edge of subscapularis, mm	6.5 ± 0.9
Distance from starting point to edge of supraspinatus, mm	4.9 ± 0.6

SD, standard deviation; *ACJ*, acromioclavicular joint; *GT*, greater tuberosity.

biceps tendon. However, to access the RI, they used a deltoid-splitting approach. Several other authors have proposed a variety of solutions. An extra-articular approach using a proximally curved nail has been described.[5] Knierim et al[10] described access medial to the acromion, which required splitting the supraspinatus muscle belly through the Neviaser portal. Park et al[19] were the first authors to describe access for a humeral nail starting point through the RI using modern straight nails. However, their approach required detaching the anterior deltoid head from the acromion with limitations in visualization of the axillary nerve during locking screw fixation.

In this article, we describe the utilitarian mini-deltopectoral dissection through which a rotator cuff–sparing approach is used for antegrade humeral IMNs. This surgical approach can be extended distally for fracture reduction and/or used if a subsequent conversion

Table III AP radiographic measurements

Radiographic measurement	Mean ± SD
Distance from starting point to medial edge of bicipital groove, mm	5.9 ± 0.3
Distance from starting point to inferior end of ACJ, mm	38.5 ± 2.3
Distance from starting point to coracoid body, mm	38.0 ± 3.5
Distance from starting point to lateral articular edge of humerus, mm	10.5 ± 1.0
Distance from starting point to subscapularis, mm	8.8 ± 0.5
Distance from starting point to supraspinatus, mm	7.4 ± 0.4
Width of humeral head on AP view, mm	54.6 ± 0.4
Distance on AP view from lateral humeral edge to starting point, mm	20.2 ± 1.5
Ratio of distance from lateral humeral edge to starting point relative to humeral head width	0.4 ± 0.0

SD, standard deviation; *ACJ*, acromioclavicular joint; *AP*, anteroposterior.

Table IV Lateral radiographic measurements

Radiographic measurement	Mean ± SD
Width of humeral head on lateral view, mm	45.1 ± 0.5
Distance on lateral view from anterior humeral edge to starting point, mm	15.7 ± 1.2
Ratio of distance from anterior humeral edge to starting point relative to humeral head width	0.3 ± 0.0

SD, standard deviation.

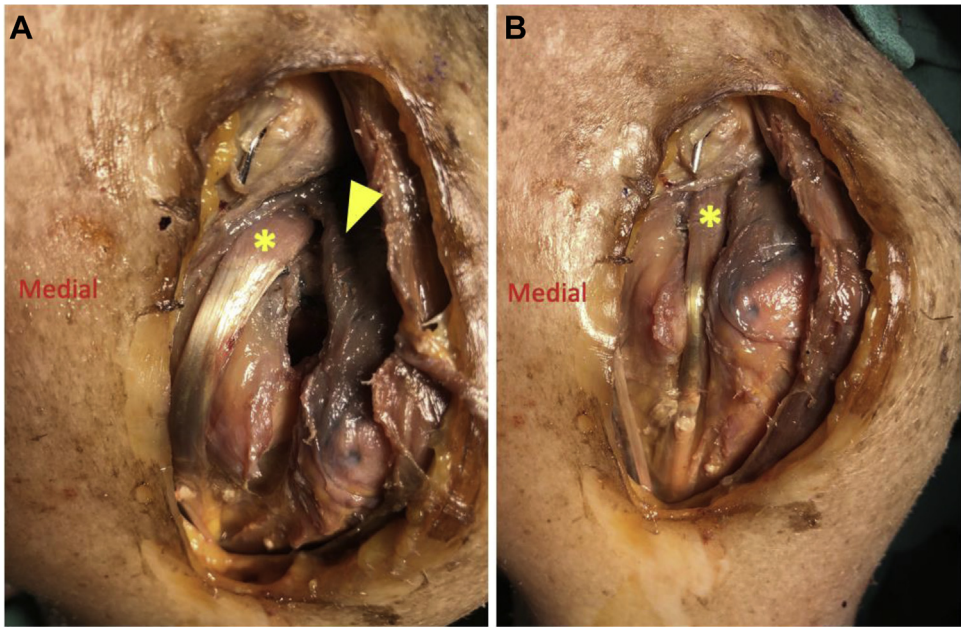

Figure 7 Images of surrounding soft tissue following humeral intramedullary nail reaming and nail placement: demonstration of biceps tendon medially dislocated (*) and integrity of rotator cuff tendon (◀) (**A**) and demonstration with biceps tendon reduced (*) (**B**).

to shoulder arthroplasty is required. This approach allows for biceps tendon preservation in younger patients who elect to avoid deformity or tenodesis or tenotomy in older patients with biceps tendon pathology. Additionally, this approach allows for proximal dissection and visualization to ensure that the starting point does not involve the rotator cuff tendon and footprint, as well as the lateral margin of the humeral head articular surface. Finally, it maximizes the exposures required to implant humeral nails.

No previous study has described the radiographic landmarks needed for antegrade humeral IMN fixation through the RI. We correlated an anatomic starting point through the RI with radiographic images. We found that the ideal starting point through the RI radiographically lies along the medial aspect of the lateral third of the humeral head on the AP view, medial to the bicipital groove (Table III). Moreover, on the lateral view, the ideal starting point radiographically lies along the posterior aspect of the anterior third of the humeral head (Table IV). The bicipital groove view, described earlier, further aided in confirming proper placement of the starting point to ensure the guidewire was sufficiently medial.

Clinical outcomes after humeral IMN fixation are varied, given differences in implant design type, surgical approach, and fracture type. In a Cochrane database review in 2011 comparing plate fixation with IMNs, no difference in outcomes was found in terms of union rate, operating time, iatrogenic radial nerve palsy, intraoperative fracture comminution, deep infection, rate of return to preinjury occupation, or functional outcome scores.[11] The authors did report a higher rate of shoulder impingement and implant removal in the nail group.

We recognize that our study is not without limitations. As with any anatomic investigation, the sample size is a limitation. A larger sample and/or inclusion of female specimens may have revealed further anatomic variability. Furthermore, measured structural distances may have minor underestimations owing to out-of-plane length contributions along the course of a given structure. For the purposes of this study, we used only intact specimens to describe the anatomic and radiographic RI starting point through a mini-deltopectoral approach. However, with fractures, additional challenges would certainly be present. Moreover, 4-part fractures with violated RIs would require adaptation of the RI humeral nail technique. Nevertheless, these limitations should not diminish the value of this attempt to correlate anatomic and radiographic analysis for an RI starting point for an antegrade humeral IMN using a mini-deltopectoral approach. Further investigation will include using a percutaneous approach to validate the reproducibility of the described radiographic landmarks. Finally, clinical investigations will be needed to confirm the efficacy of this cadaveric study and analyze unforeseen complications prior to widespread use.

Conclusion

This study demonstrates the clinical feasibility of a mini-deltopectoral approach for antegrade placement of humeral IMNs through the RI that avoids the risk of rotator cuff and humeral head articular damage. Additionally, we defined and correlated the ideal anatomic starting point with radiographic landmarks needed for antegrade humeral IMN fixation through the RI. We found that the ideal starting point through the RI radiographically lies along the medial aspect of the lateral third of the humeral head on the AP view and lies along the posterior aspect of the anterior third of the humeral head on the lateral view. Finally, the bicipital groove view can be used to confirm proper medial placement of the humeral nail starting point. Looking forward, prospective clinical studies will be critical to validate the clinical efficacy of humeral nailing through this technique.

Disclaimer

The Piedmont Orthopaedic Foundation provided a grant to complete this project. The authors, their immediate families, and any research foundations with which they are affiliated have not received any financial payments or other benefits from any commercial entity related to the subject of this article.

References

1. Baltov A, Mihail R, Dian E. Complications after interlocking intramedullary nailing of humeral shaft fractures. Injury 2014;45(Suppl 1): S9-15. https://doi.org/10.1016/j.injury.2013.10.044
2. Changulani M, Jain UK, Keswani T. Comparison of the use of the humerus intramedullary nail and dynamic compression plate for the management of diaphyseal fractures of the humerus. A randomised controlled study. Int Orthop 2007;31:391-5. https://doi.org/10.1007/s00264-006-0200-1
3. Christ AB, Gausden EB, Warner SJ, Nellestein AM, Thacher RR, Lorich DG. Rotator cuff-sparing approach for antegrade humeral nailing with biceps tenodesis: a technical trick with clinical implications. J Orthop Trauma 2017;31:e60-5. https://doi.org/10.1097/BOT.0000000000000684
4. Court-Brown CM, Caesar B. Epidemiology of adult fractures: a review. Injury 2006;37:691-7. https://doi.org/10.1016/j.injury.2006.04.130
5. Dimakopoulos P, Papadopoulos AX, Papas M, Panagopoulos A, Lambiris E. Modified extra rotator-cuff entry point in antegrade humeral nailing. Arch Orthop Trauma Surg 2005;125:27-32. https://doi.org/10.1007/s00402-004-0757-3
6. Ekholm R, Adami J, Tidermark J, Hansson K, Tornkvist H, Ponzer S. Fractures of the shaft of the humerus. An epidemiological study of 401 fractures. J Bone Joint Surg Br 2006;88:1469-73. https://doi.org/10.1302/0301-620X.88B11.17634
7. Gracitelli MEC, Malavolta EA, Assuncao JH, Kojima KE, dos Reis PR, Silva JS, et al. Locking intramedullary nails compared with locking plates for two- and three-part proximal humeral surgical neck fractures: a randomized controlled trial. J Shoulder Elbow Surg 2016;25:695-703. https://doi.org/10.1016/j.jse.2016.02.003
8. Gunther CM, Muller PE, Mutschler W, Sprecher CM, Milz S, Braunstein V. Straight proximal humeral nails are surrounded by more bone stock in comparison to bent nails in an experimental cadaveric study. Patient Saf Surg 2014;8:18. https://doi.org/10.1186/1754-9493-8-18

9. Jost B, Koch PP, Gerber C. Anatomy and functional aspects of the rotator interval. J Shoulder Elbow Surg 2000;9:336-41.
10. Knierim AE, Bollinger AJ, Wirth MA, Fehringer EV. Short, locked humeral nailing via Neviaser portal: an anatomic study. J Orthop Trauma 2013;27:63-7. https://doi.org/10.1097/BOT.0b013e31825194ad
11. Kurup H, Hossain M, Andrew JG. Dynamic compression plating versus locked intramedullary nailing for humeral shaft fractures in adults. Cochrane Database Syst Rev 2011:CD005959. https://doi.org/10.1002/14651858.CD005959.pub2
12. Lee JC, Guy S, Connell D, Saifuddin A, Lambert S. MRI of the rotator interval of the shoulder. Clin Radiol 2007;62:416-23. https://doi.org/10.1016/j.crad.2006.11.017
13. Li M, Wang Y, Zhang Y, Yang M, Zhang P, Jiang B. Intramedullary nail versus locking plate for treatment of proximal humeral fractures: a meta-analysis based on 1384 individuals. J Int Med Res 2018;46:4363-76. https://doi.org/10.1177/0300060518781666
14. Lopiz Y, Garcia-Coiradas J, Garcia-Fernandez C, Marco F. Proximal humerus nailing: a randomized clinical trial between curvilinear and straight nails. J Shoulder Elbow Surg 2014;23:369-76. https://doi.org/10.1016/j.jse.2013.08.023
15. McCormack RG, Brien D, Buckley RE, McKee MD, Powell J, Schemitsch EH. Fixation of fractures of the shaft of the humerus by dynamic compression plate or intramedullary nail. A prospective, randomised trial. J Bone Joint Surg Br 2000;82:336-9.
16. Neer CS II. Displaced proximal humeral fractures. J Bone Joint Surg Am 1970;52:1077-89.
17. Nelsen R. Heron's formula via proofs without words. Coll Math J 2001;32:290-2.
18. Palvanen M, Kannus P, Niemi S, Parkkari J. Update in the epidemiology of proximal humeral fractures. Clin Orthop Relat Res 2006;442:87-92. https://doi.org/10.1097/01.blo.0000194672.79634.78
19. Park J-Y, Pandher DS, Chun J-Y, Lee ST. Antegrade humeral nailing through the rotator cuff interval: a new entry portal. J Orthop Trauma 2008;22:419-25. https://doi.org/10.1097/BOT.0b013e318173f751
20. Plancher KD, Johnston JC, Peterson RK, Hawkins RJ. The dimensions of the rotator interval. J Shoulder Elbow Surg 2005;14:620-5. https://doi.org/10.1016/j.jse.2005.02.022
21. Sears BW, Hatzidakis AM, Johnston PS. Intramedullary fixation for proximal humeral fractures. J Am Acad Orthop Surg 2020;28:e374-83. https://doi.org/10.5435/JAAOS-D-18-00360
22. Verdano MA, Pellegrini A, Schiavi P, Somenzi L, Concari G, Ceccarelli F. Humeral shaft fractures treated with antegrade intramedullary nailing: what are the consequences for the rotator cuff? Int Orthop 2013;37:2001-7. https://doi.org/10.1007/s00264-013-2007-1
23. Wali MGR, Baba AN, Latoo IA, Bhat NA, Baba OK, Sharma S. Internal fixation of shaft humerus fractures by dynamic compression plate or interlocking intramedullary nail: a prospective, randomised study. Strategies Trauma Limb Reconstr 2014;9:133-40. https://doi.org/10.1007/s11751-014-0204-0